Recycled cyanobacteria ashes for sono-enhanced photo-Fenton wastewater decontamination

Raul Artal,[a] Laetitia Philippe,[b] Elvira Gómez,[ac] Albert Serrà[b*]

[a] Thin Films and Nanostructures Electrodeposition Group, Department of Materials Science and Physical Chemistry, Universitat de Barcelona, Martí i Franquès, 1, E-08028, Barcelona, Catalonia, Spain.

[b] Empa, Swiss Federal Laboratories for Materials Science and Technology, Laboratory for Mechanics of Materials and Nanostructures, Feuerwerkerstrasse 39, CH-3602 Thun, Switzerland.

[c] Institute of Nanoscience and Nanotechnology (IN^{2}UB), University of Barcelona, Barcelona, Catalonia, Spain.

Corresponding author: albert.serraramos@empa.ch (A.S.)

Abstract

Currently, there is massive generation of persistent organic pollutants, which are hazardous substances, owing to the exponential industrial growth and the associated waste production. Consequently, green and reliable strategies for decontaminating wastewater and generating value-added products are needed to realize the global demand of sustainability. In this study, an efficient sustainable circular process for water remediation with nearly zero residue production is developed using iron-rich cyanobacteria ashes. These cyanobacteria ashes are obtained from the combustion of *Arthrospira platensis* var lonar and are used as Fenton-like photocatalysts in different assisted photo-Fenton reactions (processes enhanced by light). The use of these iron-rich cyanobacteria ashes is particularly effective for the sono-enhanced photo-Fenton processes for water remediation (mineralization > 94.9%), with an outstanding reusability. At the end of the effective lifetime of the photocatalyst, the remaining ashes can be subsequently reused

as a supplement during the growth of new cyanobacteria, thus closing the circular process. The proposed approach is a green and sustainable process integrating both carbon dioxide fixation and clean-water production aimed at attaining sustainable development.

Keywords: remediation, mineralization, photocatalyst, Fenton, sonophoto-Fenton, microalgae ashes

Highlights

- Cyanobacteria ashes, especially iron-rich ones, are proposed as catalysts in different assisted Fenton processes.
- The use of sonication enhances the mineralization process.
- Ashes long lifetime is confirmed; no significant differences are observed after five consecutive methylene blue degradation cycles in the iron-rich cyanobacteria ashes.
- The cyanobacteria ashes can be directly recycled to produce more fresh cyanobacteria.

1. Introduction

The research on biomass is growing exponentially because it is a green, sustainable, and virtually unlimited source of carbon to produce fuels, power, heat, and value-added chemicals to address the issue of the depletion of fossil fuel resources and the increasing environmental concerns (Hu et al., 2020; Kumar et al., 2020; Zhao et al., 2019). Yearly, billions of metric tons of lignocellulose biomass from plants (phytomass) and animal biomass (zoomass) are globally produced naturally as well as a consequence of human anthropological activities (Borghei et al., 2019; Deng et al., 2016). The effective management and recycling of the produced biomass is extremely essential for reducing the adverse ecological impact, powering green circular chemistry processes, and achieving sustainable development (Deng et al., 2016; Keijer et al., 2019; Serrà et al., 2020).

In this context, cyanobacteria cultivation can significantly contribute to the development of a self-sus-

tainable process for biomass production that has promising applications in the energy–water–food–pharmaceutics nexus (Serrà et al., 2019, Solovchenko et al., 2014). Cyanobacteria have numerous potential applications in a wide range of fields, such as biopharmaceuticals, nutraceuticals, cosmetics, water decontamination, and renewable energy (Gosset et al., 2019; Wong et al., 2018; Zhang et al., 2019). They are abundant photosynthetic microorganisms and can be found in oceans, lakes, and rivers; they can endure adverse conditions, such as wastewater and broad ranges of salinity, pH, and temperature (Liao et al., 2016). Note that the cultivation of cyanobacteria in wastewater has various benefits associated with (i) the reduction in the cultivation cost, and more importantly, (ii) the phycoremediation process, which simultaneously allows the sequestration of carbon dioxide, biosorption of heavy metals, and bioaccumulation/biosorption and biotransformation of organic compounds (Kumar et al., 2020; Lebron et al., 2019; Pradhan et al., 2019; Ahmad Ansari et al., 2019). Consequently, they can be effective for water decontamination, particularly for alcohol wastewater treatment and heavy metal bioremediation. Cyanobacteria biomass can be effectively used for (i) the production of biohybrid materials for photocatalysis or absorbents (Lobakova et al., 2016), (ii) the extraction of cost-effective high-value products, such as eicosapentaenoic acid and docosahexaenoic acid (Shanab et al., 2018), and (iii) the production of supplementary food, fodder, or fertilizers (Singh et al., 2016). Importantly, cyanobacteria biomass can be combusted directly, releasing heat, or be converted to biogas or biofuels (such as bioethanol or biodiesel) (Das et al., 2018; Tsegaye et al., 2019; Zelelew et al., 2018). It is noteworthy that the solid residues obtained as a consequence of the production of bioethanol or biodiesel can be also used to produce biopellets (Serrà et al., 2020). However, in this last application, the use of biomass also has adverse effects arising from the release of a complex mixture of chemicals during combustion, which comprises of mainly carbon dioxide and also solid micro- nanoparticles (ashes), water vapor, carbon monoxide, and nitrogen oxides (Caposciutti et al., 2019; Lane et al., 2014). Consequently, the management of these residues, particularly ashes, should be addressed when proposing a green and sustainable use of cyanobacteria biomass. Note that carbon dioxide fixation occurs during the cultivation of cyanobacteria (Serrà et al., 2019).

The produced ashes not only from the combustion of biomass pellets but also from numerous other processes involving combustion, can be converted into abundant raw materials for other applications.

Such ashes have been promoted as complementary raw materials for asphalt technologies, hydrogen production, hydraulic cement, ceramic building materials, and water remediation (Alavi-Borazjani et al., 2019; Brooks et al., 2019; Molin Filho et al., 2019; Tosti et al., 2019). Furthermore, several studies have demonstrated that different types of ashes have the outstanding absorption capacities for various pollutants present in wastewater, such as organic dyes, pesticides, phenols, toxic metals, and numerous other inorganic contaminants (Johansson et al., 2016; Khodadadi et al., 2019; Yadav et al., 2014). The adsorption capacity of an ash depends strongly on its origin; therefore, detailed studies are required for individual specific industrial applications. In addition to their role as adsorbents, ashes can potentially be used as low-cost photocatalytic supports because they possess almost all the required characteristics, such as stability to light illumination, high surface area, and easy recovery (Borges et al., 2014; Katsika et al., 2018; Zeghioud et al., 2016). In addition, these ashes are inexpensive and mass-produced materials with exceptional suitability to be used in water remediation as membrane filters and photocatalysts (Borges et al., 2017; Ma et al., 2018; Ramírez-Franco et al., 2019). In particular, the cyanobacteria ashes are rich in heavy metals residues, making them potential effective Fenton-like heterogeneous catalysts for sunlight water decontamination. It is to be noted that the photo-Fenton process offers an inexpensive, sustainable, and effective process to mineralize organic compounds with the use of sunlight (Fu et al., 2018). It is well known that the mineralization of organic compounds based on the photo-Fenton process can be effectively enhanced by applying ultrasound (ultrasonically assisted catalysis or sonocatalysis) (Cetinkaya et al., 2018; Zhang et al., 2013). Sonocatalysis utilizes the advantage of the associated production of bubbles that generating localized extreme temperature and pressure conditions by the cavitation effect, leading to a high production of reactive oxygen species (ROS) (Gholami et al., 2019). Concurrently, ashes (particularly vegetal ashes) have also been revealed as effective supplements for algae culture media (Jain et al., 2013). Specifically, owing to their low cost and efficiency, heavy-metal-rich cyanobacteria ashes can allow reduction in the cyanobacteria production costs, making microalgae cultivation economically viable at the industrial scale.

Herein, we report the development of a green, sustainable, and environmentally friendly closed process (**Scheme 1**) for water decontamination using *Arthrospira platensis* (*A. platensis*) cyanobacteria-recycled biomass. The proposed process consists of three successive steps: (i) Calcination of the cyanobacteria

biomass to obtain the desired photocatalytic ashes and energy. (ii) The use of the ashes as photocatalytic substrates in Fenton, photo-Fenton, and sono-photo-Fenton reactions for sunlight-promoted degradation of persistent organic pollutants (methylene blue (MB) is selected in this study as probe). (iii) Finally, to make the process circular, the cultivation of new cyanobacteria by the reuse of the carbon dioxide, the remaining microalgae ashes, and the mineralized water obtained after the sono-enhanced photo-Fenton process. Consequently, this study focuses on investigating the viability of the reuse and recycling of one of the main wastes generated during cyanobacteria-based biofuel production (i.e., residual biomass and/or ashes). Its uses as an effective sunlight-driven photocatalyst for the mineralization of persistent organic compounds and as a supplement for the preparation of competitive culture medium supplements to grow microalgae are explored. This is aimed at minimizing waste by offering a circular green process that can have important applications in the energy–water–food–pharmaceutics nexus. The proposed circular process generates clean water while fixing carbon dioxide, releasing oxygen, and recycling the generated residues–the photocatalysts after their useful lifetimes–in an efficient closed-circle process.

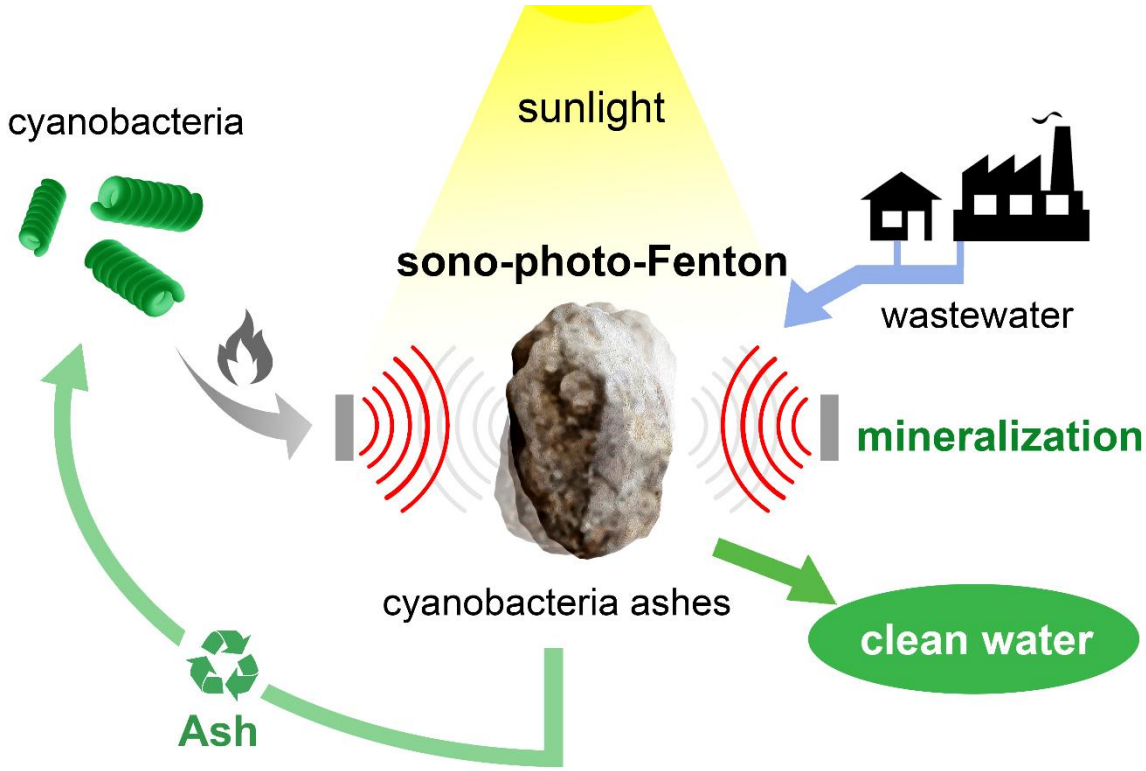

Scheme 1: Representation of the proposed circular process for water decontamination, energy production, and cyanobacteria cultivation.

2. Experimental section

2.1. Strain and culture conditions

Arthrospira platensis var lonar cyanobacteria (axenic strain – Strain No. NIVA-CYA 428) were obtained from *Espirulina* Natural Company (Catalonia, Spain). *A. platensis* were cultivated in a 30 L glass tank at 30.0 ± 0.4 °C using Zarrouk's medium (pH = 10), natural sunlight irradiation, intermittent mechanical agitation (80 rpm; 30 min-15 min on-off cycles), and air bubbling (15 min-60 min on-off cycles) (Zarrouk, 1966).

2.2. Photocatalyst preparation and characterization

Raw-cyanobacterial and iron-rich cyanobacterial ash photocatalysts were obtained after the combustion of cyanobacterial biomass in a Heraeus M110 Muffel oven (temperature of 900 °C). To obtain iron-rich ashes, cyanobacteria were immersed in a 40 ppm iron(II) chloride (> 99.0%, Sigma-Aldrich) solution (pH = 9) for 90 min under magnetic stirring (200 rpm) prior to combustion. After combustion, soluble alkaline substances and other impurities such as fibers were removed from the cyanobacterial ashes by washing repeatedly with Milli-Q water for 2 h under magnetic stirring (200 rpm) until the pH of the supernatant was equal to 7. Wash supernatants were added to the cyanobacteria tank to supplement the cultivation media. After washing, the cyanobacteria ashes were dried at 103 °C until the weight no longer changed.

The morphology and elemental composition of the cyanobacterial ashes were characterized using a field emission scanning electron microscope (FE-SEM, Hitachi S-4800) equipped with an energy-dispersive X-ray spectroscopy detector. For FE-SEM observation 100 μL of a suspension of cyanobacterial ashes (0.1 g L^{-1}) were dropped on fluorine doped tin oxide substrate and dried under nitrogen. In order to

obtain high quality FE-SEM images of cyanobacterial ashes, 4 nm of carbon was deposited on the surface of the ashes. The carbon deposition was performed using a Leica EM ACE600 sputtering system. In addition, the specific surface area was determined by the Brunauer–Emmett–Teller (BET) method from N_2 adsorption-desorption isotherms at 77 K using a Micrometrics Tristar-II. Ash elemental composition was carried out by X-ray photoelectron spectroscopy (XPS) at room temperature with a SPECS PHOIBOS 150 hemispherical analyzer (SPECS GmbH).

2.3. Water decontamination

Methylene blue (MB) (Sigma-Aldrich, > 97%) was selected as a model of a persistent organic pollutant. In order to analyze the potential of cyanobacterial ashes as photo-Fenton-like heterogeneous photocatalysts a single pollutant solution was selected. Note that this process is extensible to other organic pollutants.

Prior to initiating pollutant degradation, the adsorption capacity of the cyanobacterial ashes was investigated in dark conditions. Cyanobacterial ashes (5 mg of ashes) — both iron rich and non-iron rich — were added to 50 mL beakers containing a solution of 10 ppm methylene blue, leading to a photocatalyst dosage of 0.1 g L^{-1}. The solution pH was then adjusted to the desired value (pH = 3) using diluted sulfuric acid, and the flasks were shaken at 200 rpm for 60 min at 25 °C. At given time points, the MB concentration of the supernatant was measured by UV-vis spectroscopy.

The degradation and mineralization of MB was investigated in the presence and absence of cyanobacterial ashes in darkness, under artificial UV irradiation or solar irradiation (photocatalysis) and/or with ultrasonic irradiation (sono-catalysis), to determine the photolytic, Fenton, sono-catalytic, UV-Fenton, visible-Fenton, UV-sono-photo-Fenton, and solar-sono-photo-Fenton activities. Prior to the MB degradation assays, the organic pollutant solutions containing cyanobacterial ashes were kept in the darkroom at 25 °C for 60 min to establish adsorption-desorption equilibrium, and the solution pH was adjusted to the desired value (pH = 3) using diluted sulfuric acid. Next, the Fenton or photo-Fenton process was initiated by adding H_2O_2. All the experiments were thermostated at 20.1 ± 0.2°*C* and maintained under magnetic stirring (400 rpm). **Table 1** summarizes the degradation and mineralization conditions used in

each experiment. In all assays, MB degradation was tracked across a 100-min reaction period by UV-vis spectroscopy. The catalyst dosage and H_2O_2 concentration were selected based on literature regarding Fenton and photo-Fenton mineralization of MB (Ahmed et al., 2016).

Experiment	**Ashes / g L^{-1}**	**H_2O_2 / mM**	**Light Irradiation**	**US irradiation**
Photolysis	-	-	UV or Solar	-
Fenton	0.1	10	-	-
Sono-catalysis	0 or 0.1	-	-	300 W 40 kHz
Photo-Fenton	0.1	10	UV or Solar	-
Sono-Photo-Fenton	0.1	10	UV or Solar	300 W 40 kHz

Table 1: Conditions of the MB degradation/mineralization experiments.

The photo-Fenton experiments used either an 8W mercury lamp with a wavelength of 365 nm (light intensity of 1.4 W m^{-2}) or natural sunlight (average light intensity 1.5 W m^{-2}). Sonocatalytic experiments employed an UCE ultrasonic generator (nominal power: 300 W; frequency: 40 kHz).

Water decontamination analysis: The photodegradation of MB was determined by UV-vis spectroscopy (UV-1800 spectrophotometer, Shimadzu) at a wavelength of $\lambda_{max} = 662$ nm in a quartz cuvette with an optical path length of 1 cm. Each experiment was performed in triplicate under identical conditions. The pollutant mineralization was measured as the abatement of total organic carbon (TOC) after the 100-min reaction period, determined on a Shimadzu V_{CSH} analyzer.

Catalyst reusability: To evaluate photocatalyst stability, recyclability, and reusability, the microalgal ashes were collected and reused for the degradation of 10 ppm MB over five consecutive cycles (UV-sonophoto-Fenton conditions only). After the fifth cycle, the morphological stability of the recycled microalgal ashes was examined by FE-SEM.

2.4. Recyclability of photocatalysts

After the photocatalysts lifetime, cyanobacteria ashes were recycled as a supplement for Zarrouk's cyanobacteria media in the cultivation medium of *A. platensis* var lonar cyanobacteria. The following three cultivation media have been prepared:

Medium	**Composition**
Zarrouk's medium	100% (v/v) Zarrouk's medium
Raw-cyanobacterial ashes	20% (v/v) Zarrouk's medium + 80% (v/v) recycled raw-cyanobacterial ash suspension (i.e., 1 g of ash per L of water)
Iron-rich cyanobacterial ashes	20% (v/v) Zarrouk's medium + 80% (v/v) recycled iron-rich cyanobacterial ash suspension (i.e., 1 g of ash per L of water)

Table 2: Composition of the three cyanobacteria media.

During the recycling experiments, the cultivation tank was set at 30.0 ± 0.4°C and subjected to natural sunlight irradiation, intermittent mechanical agitation at 80 rpm in two 30- and 15-min on-off cycles, followed by air bubbling in two 15- and 60-min on-off cycles. *A. platensis* grew mixotrophically in these three tested media over a thirteen-day period.

Dry biomass determination: Each day, three 20 mL samples were extracted from each microalgae cultivation tank and filtered through pre-weighed GF/F Whatman® glass microfiber filters (WHA1825021, Sigma-Aldrich), which were then dried in an oven at 40 °C and weighed. Biomass production was calculated as mg of dry biomass per L of cultured media.

Photosynthetic pigments determination: Chlorophyll-a, and carotenoids concentrations in the cyanobacterial biomass cultivated in these three culturing conditions were spectroscopically measured using the Lichtenthaler and Wellburn method (Wellburn, et al., 1984; Lichtenthaler, 1987). When the stationary growth phase was reached, three 5-mL samples from each culture tank were centrifuged at 5,000 rpm for 10 min and later washed with phosphate-buffered saline (PBS, (i.e., 0.01 M of phosphate buffer, 0.0027 M of KCl, and 0.137 M of NaCl, pH 7.4) solution three times. Once the supernatant was discarded, ethanol (96% v/v) was thoroughly mixed in to the cyanobacteria residues, after which the pigments were extracted in ethanol at 65 °C for 90 min. Next, the absorbance of the supernatant in the

ethanol solution at 470, 649, and 665 nm was measured using a UV-1800 Shimadzu UV–vis spectrophotometer (Shimadzu Corporation). Chlorophyll-a and carotenoids concentrations were calculated as mg L^{-1}.

Glycogen determination: Glycogen was mechanically extracted from the cyanobacteria of three samples of these three different culturing conditions in cold PBS using a laboratory homogenizer at 20,000 rpm for 3 min. Next, homogenates were centrifuged at 13,000 rpm at 4°C for 10 min, and supernatants were recovered for glycogen analysis and filtered through 0.2-µm syringe filters. Glycogen content was determined using a glycogen assay kit (#MAK016, Sigma-Aldrich), and the analysis was performed in triplicate.

3. Results and Discussion

In this study, the cyanobacteria ashes obtained during the thermochemical conversion of cyanobacterial biomass into energy are used for the efficient mineralization of persistent organic pollutants and following recycling for the effective integration of cyanobacteria cultivation. This is a green circular process (**Scheme 1**), aiming to prevent the production of any type of waste. To realize this, the residues produced in each individual step of this process should be used or recycled in the following one, introducing the concept of clean production as an approach to increase the efficiency of the use of energy, water, and natural resources. The thermal process of combustion converts mass, in this case dried cyanobacterial biomass, to energy while producing both gas (mainly carbon dioxide) and solid residue (cyanobacterial ashes). The produced carbon dioxide can be readily fixed during cyanobacteria cultivation, improving biomass production. Consequently, this study focuses on the reutilization of the ashes generated during the combustion of cyanobacterial biomass, first for the sono-enhanced photo-Fenton mineralization of persistent organic pollutants and second for the further cultivation of microalgae.

According to ISO 17225-6:2014 standard for non-woody pellets, cyanobacteria biomass can be considered as a commercial biofuel for the fabrication of non-woody pellets provided the following requirements are met: ash content < 10 wt. %, moisture content < 15 wt. %, and calorific power > 14,5 MJ kg^{-1}.

We recently demonstrated that *A. platensis* var lonar pellets comply with the abovementioned requirements (ash content < 6 wt. %, moisture content < 6 wt. %, calorific power ≈ 20,6 MJ kg^{-1}). Therefore, we utilize A. *platensis* var lonar as the source of biomass both for the combustion and recycling of the residual products (Serrà et al., 2019).

3.1. Photocatalyst preparation and characterization

The potential of cyanobacterial ashes as heterogeneous Fenton-like photocatalysts was explored in this study. Raw- and iron-rich- cyanobacterial ashes were fabricated by the calcination of cyanobacterial biomass in the presence of oxygen. The iron-rich cyanobacteria biomass was easily obtained after dipping the biomass for 90 min in an alkaline solution (pH = 9) containing 40 ppm iron (II) chloride. Prior to the synthesis of the iron-rich cyanobacterial ashes, Fourier-transform infrared spectroscopy was conducted to identify the main functional groups of the *A. platensis* cell wall, to select the most adequate pH for the promotion of the biosorption of ions. Note that biosorption can involve complex mechanisms, such as ion exchange, microprecipitation, and electrostatic attraction. Specifically, the main biosorption mechanisms for the metal ion removal by cyanobacteria are ion exchange, microprecipitation, and metal ion interaction with the functional groups of the cyanobacteria surface. As expected, the Fourier-transform infrared spectra (**Figure 1**) of dried *A. platensis* biomass revealed the presence of amino, carboxyl, hydroxyl, phosphate, and sulfate moieties as the main functional groups. This was because the main components of its cell wall are teichuronic acid, teichoic acid, polysaccharides, and proteins. Consequently, the biosorption of iron ions may be higher in alkaline conditions owing to the non-protonation of the negatively charged functional groups.

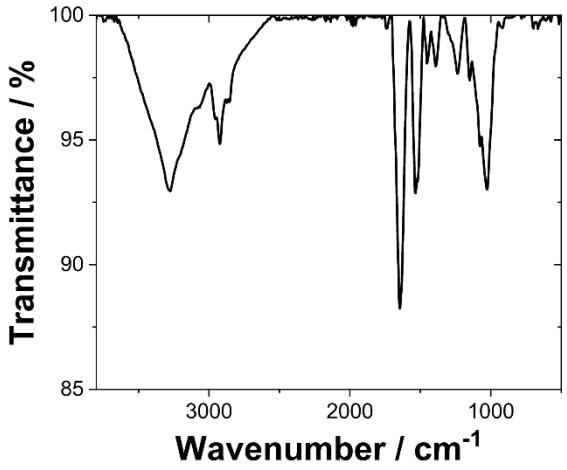

Figure 1: Fourier-transform infrared spectra of the A. *platensis* var lonar biomass.

Once the cyanobacteria were calcined, the presence of iron bioaccumulation was readily notable by the naked eye based on the color of the obtained ashes (**Figures 2a** and **b);** the raw *A. platensis* ashes presented a burly-wood color, whereas the iron-rich *A. platensis* ashes were black. Importantly, the differences in the absorption spectra (**Figure 2c** and **d**) of the raw- and iron-rich cyanobacterial ashes demonstrated the significant effect metallic impurities (i.e., iron ions) had on the calcination process. Note that the optoelectronic properties, and consequently the color, are significantly affected by the particle size, shape, crystal defects, impurities, and other factors.

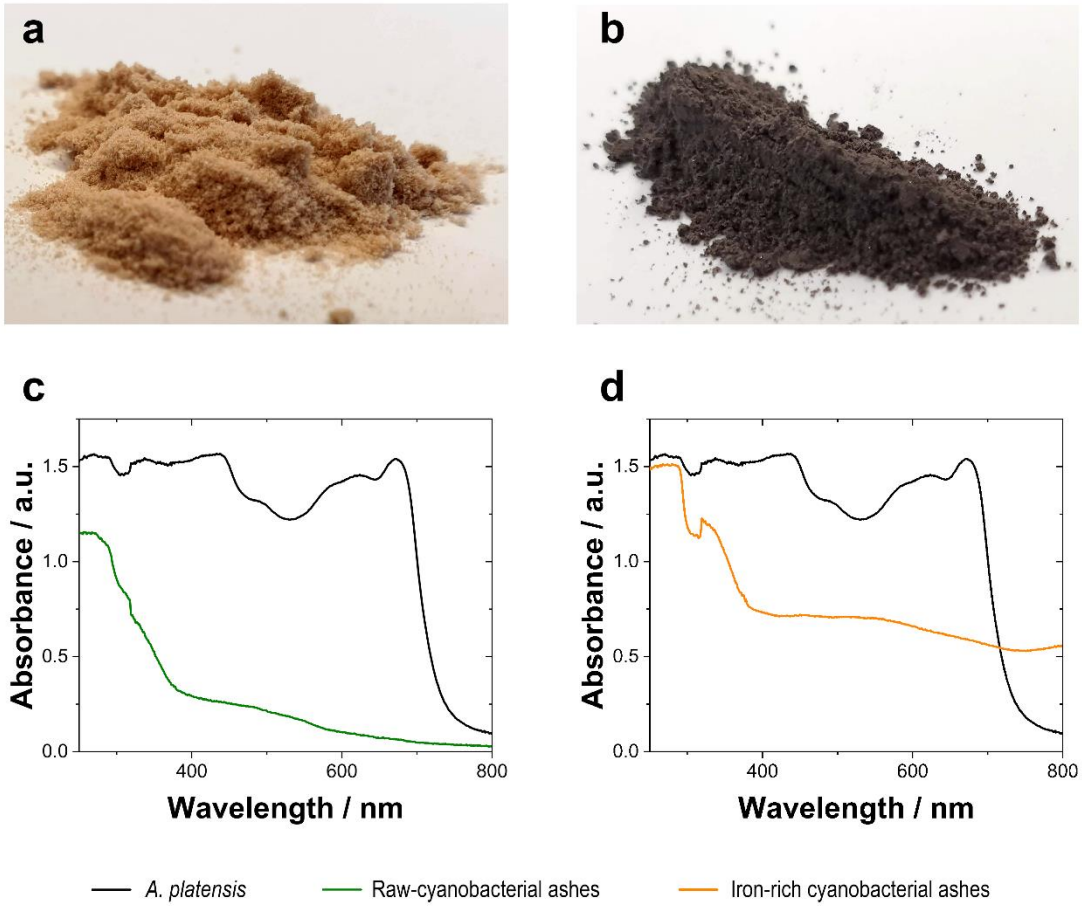

Figure 2: Photographs of the (a) raw-cyanobacterial ashes and (b) iron-rich cyanobacterial ashes; UV-vis absorption spectra of the (c) raw-cyanobacterial and (d) iron-rich cyanobacterial ashes.

The observed morphology of the cyanobacterial ashes presented that they consisted of non-spherical, irregularly-shaped microparticles ranging in size from approximately 1 to 50 µm. Further, they were composed of various aggregates (e.g., rods, geometric sheets) (**Figure 3)**, offering openings and high porosity, and the Brunauer–Emmett–Teller (BET) surface areas of the raw-microalgal ashes and iron-rich cyanobacterial ashes were high, 21.3 and 24.9 $m^2 g^{-1}$, respectively. The morphologies and BET surface areas obtained for both the types of ashes support the use of cyanobacterial ash-based photo-catalysts as Fenton-like heterogeneous photocatalysts to promote the elimination of persistent organic pollutants from wastewater.

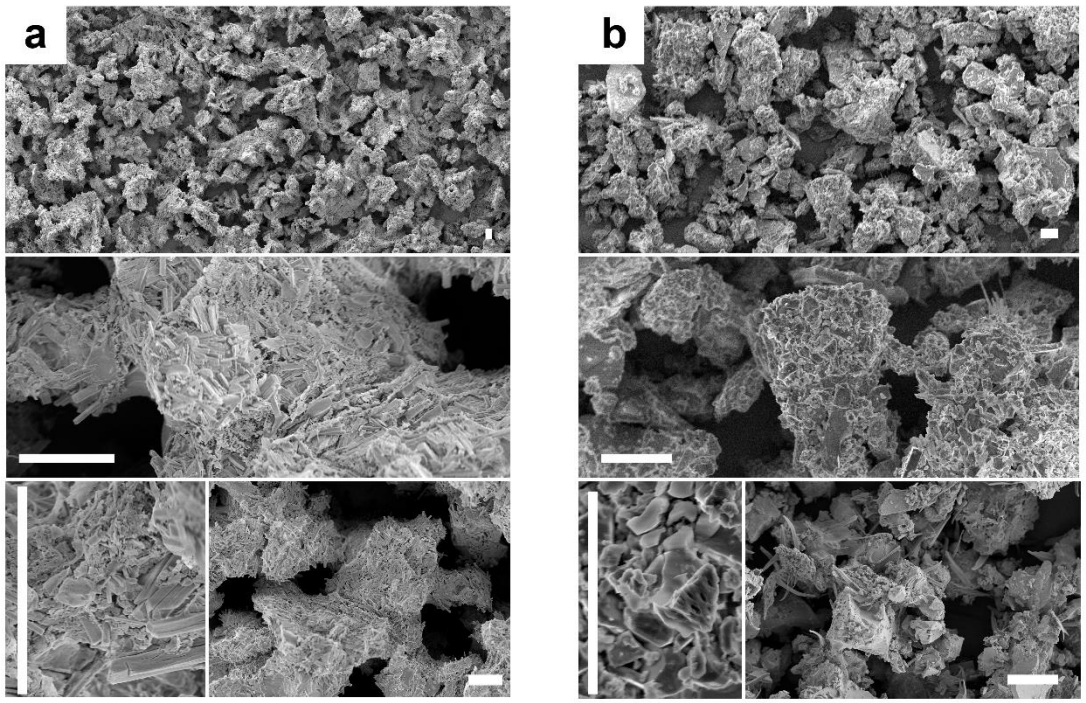

Figure 3: Field emission scanning electron microscopy (FE-SEM) micrographs of the (a) raw-cyanobacterial and (b) iron-rich cyanobacterial ashes. Scale bar: 10 µm.

The chemical compositions of the cyanobacterial ashes (**Table 2**) are fundamental for their application as Fenton-like heterogeneous photocatalysis; this is because photocatalytic activity can be strongly affected by other metals. For example, the Fenton process is limited in presence of Ni(II) ions and contrastingly is synergistically promoted in the presence of Co(II) or Mn(II) ions. Note that the iron content of the iron-rich cyanobacterial ashes was about six times higher than that of the raw-cyanobacterial ashes (**Table 3**).

	Raw-cyanobacterial ashes	**Iron-rich cyanobacterial ashes**
Fe / mg g^{-1}	48±3	256±4
Mg / mg g^{-1}	12.4 ± 0.5	12.2 ± 0.3
Al / mg g^{-1}	23 ± 2	21 ± 1
Si / mg g^{-1}	64 ± 3	63 ± 2
P / mg g^{-1}	12 ± 2	14 ± 2

S / mg g^{-1}	16 ± 2	19 ± 3
Ca / mg g^{-1}	51 ± 4	55 ± 2
Mn / mg g^{-1}	18 ± 2	18 ± 3
N / mg g^{-1}	24 ± 3	23 ± 3

Table 3: Chemical composition of raw-cyanobacterial and iron-rich cyanobacterial ashes.

3.2. Water decontamination

Prior to the use of the cyanobacterial ashes as Fenton-like catalysts, their adsorption capacities (under dark conditions) were evaluated to establish the adsorption-desorption equilibrium time sustainable. The results (**Figure 4**) revealed that the percentage of MB adsorption was higher for the iron-rich cyanobacterial ashes (9 %) than that for the raw-cyanobacterial ashes (5%). For both types of ashes, the adsorption-desorption equilibrium was attained after 30 min of immersion.

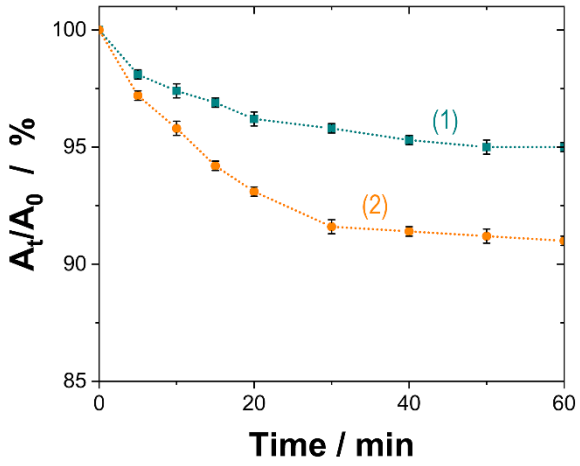

Figure 4: Adsorption of MB (10 ppm solution) at 25.0 ± 0.1 ºC in the presence of (1) the raw-cyanobacterial ashes and (2) the iron-rich cyanobacterial ashes. The error bars indicate the standard deviations from three replicate experiments.

The aim of this process was the decontamination of wastewater by the total mineralization of persistent organic pollutants (in this case MB), which included total conversion into carbon dioxide, water, and inorganic species. This was achieved by catalysis of Fenton process by raw-cyanobacterial ash and iron-

rich cyanobacterial ash-based photocatalysts under UV and sunlight irradiation assisted by sonication. The mineralization process is based on the classical Fenton reaction as follows:

$$Fe^{2+} + H_2O_2 \rightarrow Fe^{3+} + HO^{\cdot} + OH^{-} \quad (1)$$

Note that hydroxyl radicals (HO•), which are powerful non-selective oxidants, are produced by the reaction between Fe(II) and hydrogen peroxide (H_2O_2) (Pignatello et al., 2007; Brillas et al., 2009). Irradiation with light, particularly ultraviolet A light ($315 < \lambda > 400$), is known to accelerate mineralization, mainly by promoting the photolysis of $Fe(OH)^{2+}$ (the predominant Fe(III) species in aqueous solutions at pH 3) and consequently regenerating the Fe(II) catalyst to produce more hydroxyl radicals. This is known as the photo-Fenton reaction (Pignatello et al., 2007; Brillas et al., 2009). The additional use of sonication induces the formation of localized bubbles in the solution, called as *hot spots*, where the extreme conditions of pressure and temperature can favor the mineralization (Naddeo et al., 2012). In homogeneous Fenton processes, the removal of the iron ions introduced during mineralization is expensive in terms of the reagents and time required. However, Fenton-like processes can be performed using heterogeneous Fenton-like catalysts, which can be easily removed and re-used. Therefore, the utilization of cyanobacterial ashes as heterogeneous Fenton-like photocatalysts was evaluated for the mineralization of (MB).

Figure 5 shows the efficiencies of the photolytic, Fenton, sono-catalytic, UV-Fenton, visible-Fenton, UV-sonophoto-Fenton, and solar-sonophoto-Fenton degradation processes, over 100 min of irradiation, achieved using UV-vis spectroscopy as the determination method. In addition, the mineralization established by measuring the reduction in the total organic content (TOC) after 100 min of irradiation is summarized in **Table 4**. This table emphasizes that the photolytic degradation of MB under UV and natural sunlight irradiation is practically negligible (< 2%).

	Raw-cyanobacterial ash			Iron-rich cyanobacterial ash		
	MB degradation / %		Mineralization (100 min) / %	MB degradation / %		Mineralization (100 min) / %
	20 min	100 min		20 min	100 min	
Sono-catalysis	3.6±1.3	13.2±1.6	9.2±0.3	3.4±1.3	16.2±1.4	11.3±0.3
Fenton	5.3±1.2	9.6±1.8	5.5±0.2	15.3±1.3	23.9±1.1	16.2±0.2
UV-Photo-Fenton	68.8±2.3	96.1±0.9	64.5±0.4	89.4±2.1	99.0±0.2	86.5±0.4
Solar-Photo-Fenton	60.5±2.3	90.3±0.3	61.2±0.2	68.7±2.4	94.7±0.2	79.1±0.2
UV-Sonophoto-Fenton	94.1±2.2	99.0±0.6	71.4±0.3	97.8±1.3	99.3±0.2	96.1±0.4
Solar-Sonophoto-Fenton	86.8±2.5	99.1±0.2	71.4±0.1	92.4±1.2	99.9±0.1	94.9±0.5

Table 4: Photocatalytic MB (10 ppm) degradation of 0.1 g L^{-1} raw-cyanobacterial ashes or iron-rich cyanobacterial ashes at 20 ºC.

Under silent conditions (non-sonification conditions), after 100 min of UV (UV-photo-Fenton) and natural sunlight (solar-photo-Fenton) irradiation, 96.1% and 90.3% degradation is realized with the raw-cyanobacterial ashes and slightly higher degradation of 99.0% and 94.7% is attained by the iron-rich cyanobacterial ashes, respectively. Note that after 20 min, the photodegradation of MB by the raw-cyanobacterial ashes is significantly lower, dropping to 68.8% and 60.5% under UV (UV-photo-Fenton) and natural sunlight (solar-photo-Fenton) irradiation, respectively. Concurrently, when the iron-rich cyanobacterial ashes were used, after 20 min, comparatively higher degradation was achieved (89.4% and 68.7% under UV and natural sunlight irradiation, respectively). As expected, the same trend was observed from the mineralization values, which are determined at a particular time that is slightly prior to the occurrence degradation, owing to the complexity of the mineralization process. Comparing the performances of the two ash types, the consistently higher efficiencies of the iron-rich ashes are explained by their higher iron content, which enhances the generation of hydroxyl radicals and consequently promotes the oxidation of the pollutants (here MB). The high values obtained with the iron-rich ashes under sunlight irradiation confirm the suitability of their potential use for decontamination, evidencing that the use of a zero-cost light source is preferable over the cost and energy consumption of a UV-generating lamp.

Under sonication, the effect of the *hot spots* becomes notable with the increased mineralization achieved by both the UV-sono-photo-Fenton and solar-sono-photo-Fenton processes. With sonication, after the first 20 min of irradiation, the MB degradation is 94.1% and 86.8% for the raw-cyanobacterial ashes and slightly higher at 97.8% and 92.4% for the iron-rich cyanobacterial ashes under UV and sunlight irradiation, respectively. Note that these degradation values are similar to those obtained after 100 min of irradiation in the photo-Fenton experiments without sonication, which demonstrates that sonication significantly enhances the kinetics of MB degradation. Similar behavior is observed in the evaluation of the mineralization after 100 min, which reaches 71.4% for the raw-cyanobacterial ashes under both the irradiation conditions and 96.1% and 94.9% for the iron-rich cyanobacterial ashes under UV and solar light irradiation, respectively.

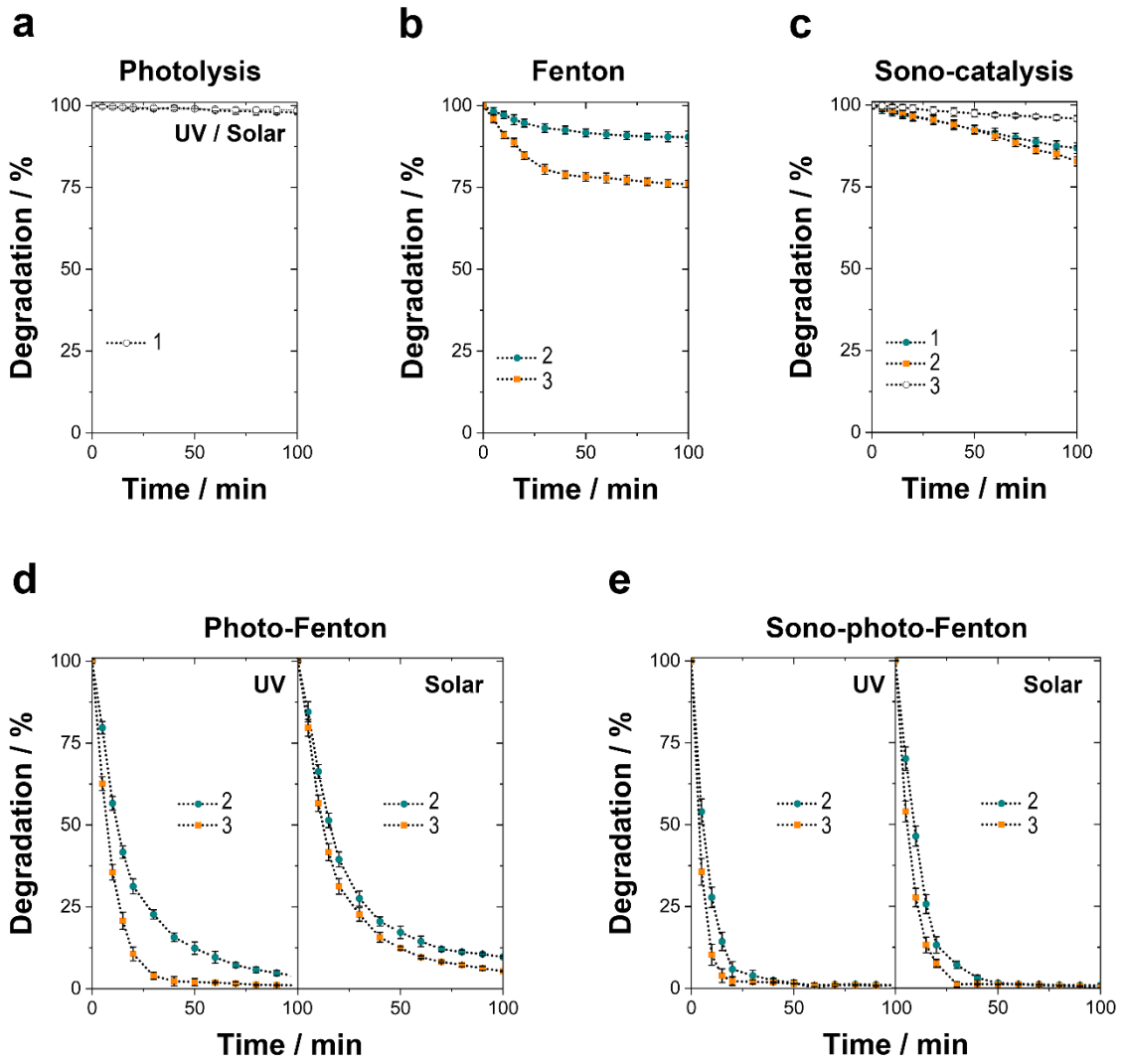

Figure 5: Photolytic, Fenton, sonocatalytic, photo-Fenton, and sonophoto-Fenton degradation of MB (10 ppm solution) at 25.0 ± 0.1 ºC in the (1) absence of any catalyst and in the presence of (2) the raw-cyanobacterial ashes and (3) iron-rich cyanobacterial ashes. The error bars indicate the standard deviations from four replicate experiments.

The mineralization attained with the bare sono-catalysis and bare-Fenton processes are significantly lower than that realized by the photo- or sonophoto- Fenton processes, which illustrates their effectiveness, particularly of the sonophoto-Fenton processes, for the mineralization of persistent organic pollutants. Additionally, the iron-rich cyanobacterial ashes result in higher degradation and mineralization

than the raw-cyanobacterial ashes, confirming that iron content synergistically increases the efficiencies of Fenton-based processes.

3.3. Photocatalyst reusability for water decontamination

The stability and reusability of the cyanobacterial ashes were evaluated by reusing the catalyst over five consecutive MB degradation cycles (**Figure 6a**) under UV irradiation. No significant differences were observed in the MB photodegradation across all the successive runs, and a degradation of approximately 99% was achieved even after five runs. Furthermore, the imaging of the ashes after the runs did not present morphological changes after the five successive MB degradation cycles (**Figure 6b** and **6c**). Consequently, the iron-rich cyanobacterial ashes can be easily reused for the mineralization of persistent organic pollutants, providing a new application for cyanobacterial ash residues. The robustness of the cyanobacterial ashes allows their reuse without the loss of their catalytic activity. Furthermore, the application of sonication, which is an aggressive treatment prohibited for other heterogeneous catalysts, does not damage the ashes and enhances the kinetics of the degradation and mineralization processes.

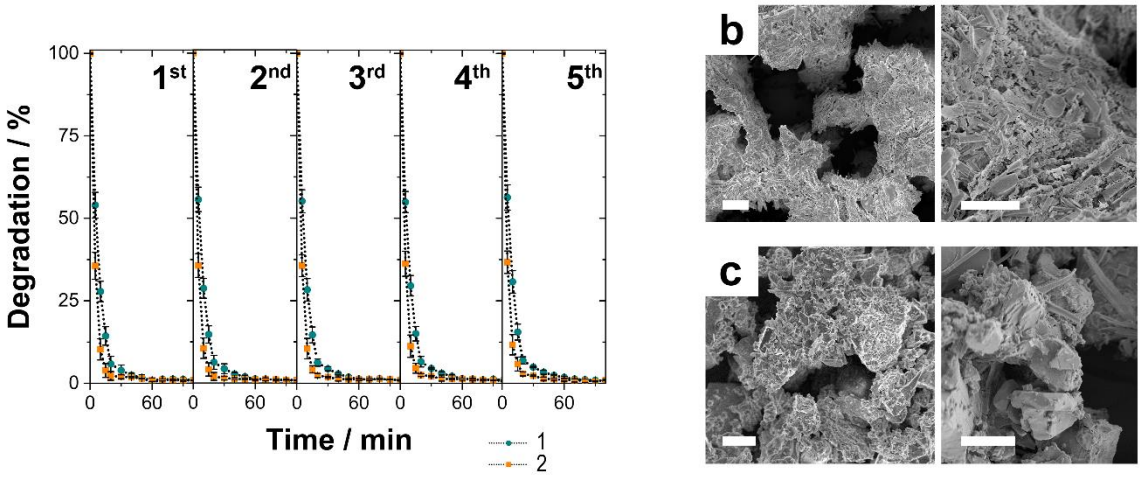

Figure 6: (a) UV-sonophoto-Fenton reusability over five cycles of use of (1) the raw-cyanobacterial ashes and (2) the iron-rich cyanobacterial ashes to degrade 10 ppm MB. The FE-SEM micrographs after the fifth cycle for (b) the raw-cyanobacterial ashes and (c) the iron-rich cyanobacterial ashes. Scale bar: 10 µm.

3.4. Recyclability of cyanobacterial ashes

Attending to reduce the production of residues after the effective lifetime of the ashes used in catalytic purposes the application of these inactive-cyanobacterial ashes is proposed as a tool to close the cycle. The proposed cultivation of *A. platensis* var lonar supposes the fixation of the carbon dioxide produced both during the combustion of the cyanobacteria pellets and on the mineralization of persistent organic pollutants. Furthermore, it assumes the incorporation of the remaining cyanobacterial ashes used as photocatalysts as supplements for the growth of fresh *A. platensis*. Note that moderate carbon dioxide levels when artificially injected during cultivation can effectively benefit cyanobacterial biomass growth. As displayed in **Figure 7**, both types of the ashes used are demonstrated to be suitable for the cultivation of additional cyanobacteria biomass. Furthermore, the utilization of an ash-based medium moderately enhances cyanobacterial biomass production compared to that achieved using only Zarrouk's medium. However, after 11 days, there are no differences in the stationary growth phases in the different tested culture media.

Finally, to analyze the quality of the cyanobacterial biomass produced using these three different cultivation media, the contents of glycogen, chlorophyll-a, and carotenoids were determined. The glycogen, chlorophyll-a, and carotenoids contents in the cyanobacteria cultivated in Zarrouk's medium were approximately 21 wt. %, 8 wt. %, and 0.1 wt. %, respectively. Those in the cyanobacteria cultivated in the raw-cyanobacterial ash-based medium and iron-rich cyanobacterial ash-based medium were 70 wt. %, 3.5 wt. % and 0.4 wt. %, respectively. Note that the chemical composition of cyanobacteria strongly depends on the culture media composition. However, the higher glycogen content, which is generally obtained in a nitrate-deficient Zarrouk's medium, can be beneficial for other applications of microalgae, such as bioethanol production (Serrà et al., 2019).

Thus, with this step closing the cycle, a zero residue process was successfully developed for the simultaneous elimination of persistent organic pollutants in wastewater and production of microalgae biomass.

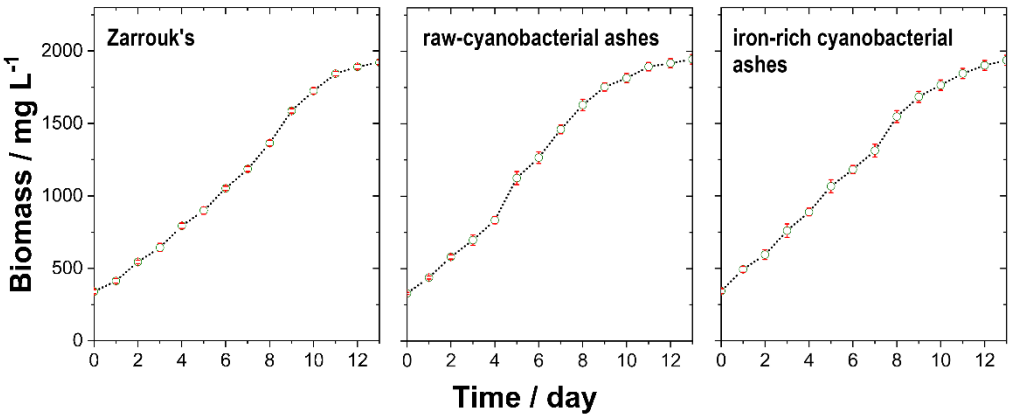

Figure 7: Cyanobacterial biomass production in Zarrouk's medium, the raw-cyanobacterial ash-based medium, and the iron-rich cyanobacterial ash-based medium.

4. Conclusions

In this study, tests were performed to explore the use of the residues generated during the combustion of cyanobacteria pellets as catalysts in different assisted Fenton processes. Two types of ashes with different iron contents were evaluated, demonstrating that in all the cases a higher iron content favored degradation and mineralization.

The iron-rich cyanobacteria ashes exhibited outstanding photocatalytic activity for persistent organic pollutants (e.g., MB) mineralization under sunlight irradiation and sonication, with an extended effective lifetime leading to an efficient strategy for water remediation. Combining radiation and sonication enhanced the Fenton process, particularly using the iron-rich ashes, under which conditions the mineralization reached values similar to those of degradation near 100%, making it evident that a quasi-complete remediation process of the wastewater occurred. The ashes maintained their efficiency during consecutive cycles without losing their capability. The experiments using the more efficient iron-rich microalgae ashes as photocatalysts demonstrated a long activity period and high reusability.

In addition, the carbon dioxide released during the mineralization and with the remaining ash residue could be exploited for cultivation of fresh cyanobacteria, closing the circular process.

In summary, a green circular closed process using iron-rich microalgae ashes from *A. platensis var lonar* was developed for MB remediation in wastewater with nearly zero-residue production. Thus, the use of iron-rich cyanobacteria ashes as Fenton-like photocatalysts enables a green and sustainable process that integrates carbon dioxide fixation and clean-water production.

ACKNOWLEDGMENT

The work leading to these results has received funding from Metrohm foundation, the TEC2017-85059-C3-2-R projects (co-financed by the *Fondo Europeo de Desarrollo Regional*, FEDER) from the Spanish *Ministerio de Economía y Competitividad* (MINECO). Albert Serrà would like to acknowledge funding from the EMPAPOSTDOCS-II program. The EMPAPOSTDOCS-II programme has received funding from the European Union's Horizon 2020 research and innovation programme under the Marie Skłodowska-Curie grant agreement number 754364.

References

Ahmed, Y., Yaakob, Z., Akhtar, P., 2016. Degradation and mineralization of methylene blue using a heterogeneous photo-Fenton catalyst under visible and solar light irradiation. Catal. Sci. Technol. 6, 1222–1232. https://doi.org/10.1039/c5cy01494h

Alavi-Borazjani, S.A., Capela, I., Tarelho, L.A.C., 2019. Dark fermentative hydrogen production from food waste: Effect of biomass ash supplementation. Int. J. Hydrogen Energy 44, 26213–26225. https://doi.org/10.1016/j.ijhydene.2019.08.091

Ansari, F.A., Ravindran, B., Gupta, S.K., Nasr, M., Rawat, I., Bux, F., 2019. Techno-economic estimation of wastewater phycoremediation and environmental benefits using Scenedesmus obliquus microalgae. J. Environ. Manage. 240, 293–302. https://doi.org/10.1016/j.jenvman.2019.03.123

Borges, M.E., Hernández, T., Esparza, P., 2014. Photocatalysis as a potential tertiary treatment of urban wastewater: new photocatalytic materials. Clean Technol. Environ. Policy 16, 431–436. https://doi.org/10.1007/s10098-013-0637-z

Borges, M.E., Sierra, M., Esparza, P., 2017. Solar photocatalysis at semi-pilot scale: wastewater decontamination in a packed-bed photocatalytic reactor system with a visible-solar-light-driven photocatalyst. Clean Technol. Environ. Policy 19, 1239–1245. https://doi.org/10.1007/s10098-016-1312-y

Borghei, M., Lehtonen, J., Liu, L., Rojas, O.J., 2018. Advanced Biomass-Derived Electrocatalysts for the Oxygen Reduction Reaction. Adv. Mater. 30, 1–27. https://doi.org/10.1002/adma.201703691

Brillas, E., Sirés, I., Oturan, M.A., 2009. Electro-fenton process and related electrochemical technologies based on fenton's reaction chemistry. Chem. Rev. 109, 6570–6631. https://doi.org/10.1021/cr900136g

Brooks, A.L., Shen, Z., Zhou, H., 2019. Development of a high-temperature inorganic synthetic foam with recycled fly-ash cenospheres for thermal insulation brick manufacturing. J. Clean. Prod. 118748. https://doi.org/10.1016/j.jclepro.2019.118748

Caposciutti, G., Barontini, F., Galletti, C., Antonelli, M., Tognotti, L., Desideri, U., 2019. Woodchip size effect on combustion temperatures and volatiles in a small-scale fi xed bed biomass boiler. Renew. Energy. https://doi.org/10.1016/j.renene.2019.11.005

Cetinkaya, S.G., Morcali, M.H., Akarsu, S., Ziba, C.A., Dolaz, M., 2018. Comparison of classic Fenton with ultrasound Fenton processes on industrial textile wastewater. Sustain. Environ. Res. 28, 165–170. https://doi.org/10.1016/j.serj.2018.02.001

Das, S.K., Sathish, A., Stanley, J., 2018. Production of Biofuel and Bioplastic from Chlorella Pyrenoidosa. Mater. Today Proc. 5, 16774–16781. https://doi.org/10.1016/j.matpr.2018.06.020

Deng, J., Li, M., Wang, Y., 2016. Biomass-derived carbon: Synthesis and applications in energy storage and conversion. Green Chem. 18, 4824–4854. https://doi.org/10.1039/c6gc01172a

Fu, H., Zhou, Z., Zheng, S., Xu, Z., Alvarez, P.J.J., Yin, D., Qu, X., Zhu, D., 2018. Dissolved Mineral Ash Generated by Vegetation Fire Is Photoactive under the Solar Spectrum. Environ. Sci. Technol. 52, 10453–10461. https://doi.org/10.1021/acs.est.8b03010

Gholami, P., Khataee, A., Soltani, R.D.C., Bhatnagar, A., 2019. A review on carbon-based materials for heterogeneous sonocatalysis: Fundamentals, properties and applications. Ultrason. Sonochem. 58, 104681. https://doi.org/10.1016/j.ultsonch.2019.104681

Gosset, A., Oestreicher, V., Perullini, M., Bilmes, S.A., Jobbagy, M., Dulhoste, S., Bayard, R., Durrieu, C., 2019. Optimization of sensors based on encapsulated algae for pesticide detection in water. Anal. Methods. https://doi.org/10.1039/C9AY02145K

Hu, Y., Gong, M., Xing, X., Wang, H., Zeng, Y., Xu, C.C., 2020. Supercritical water gasification of biomass model compounds: A review. Renew. Sustain. Energy Rev. 118, 109529. https://doi.org/10.1016/j.rser.2019.109529

Jain, S., Singh, S.G., 2013. Low cost medium formulation using cow dung ash for the cultivation of cyanobacterium: Spirulina (Arthrospira) platensis. Emirates J. Food Agric. 25, 682–691. https://doi.org/10.9755/ejfa.v25i9.16394

Johansson, C.L., Paul, N.A., de Nys, R., Roberts, D.A., 2016. Simultaneous biosorption of selenium, arsenic and molybdenum with modified algal-based biochars. J. Environ. Manage. 165, 117–123. https://doi.org/10.1016/j.jenvman.2015.09.021

Katsika, E., Moutsatsou, A., Karayannis, V., Volioti, M., Tsoukleris, D., 2018. Synthesis and characterization of lignite fly ash ceramic substrates coated with TiO2 slurry, and evaluation in environmental applications. J. Aust. Ceram. Soc. 54, 711–719. https://doi.org/10.1007/s41779-018-0201-8

Keijer, T., Bakker, V., Slootweg, J.C., 2019. Circular chemistry to enable a circular economy. Nat. Chem. 11, 190–195. https://doi.org/10.1038/s41557-019-0226-9

Khodadadi, M., Al-Musawi, T.J., Kamranifar, M., Saghi, M.H., Hossein Panahi, A., 2019. A comparative study of using barberry stem powder and ash as adsorbents for adsorption of humic acid. Environ. Sci. Pollut. Res. 26, 26159–26169. https://doi.org/10.1007/s11356-019-05879-4

Kumar, B., Bhardwaj, N., Agrawal, K., Chaturvedi, V., Verma, P., 2020. Current perspective on pretreatment technologies using lignocellulosic biomass: An emerging biorefinery concept. Fuel Process. Technol. 199. https://doi.org/10.1016/j.fuproc.2019.106244

Kumar, R., Ghosh, A.K., Pal, P., 2020. Synergy of biofuel production with waste remediation along with value-added co-products recovery through microalgae cultivation: A review of membrane-integrated green approach. Sci. Total Environ. 698. https://doi.org/10.1016/j.scitotenv.2019.134169

Lane, D.J., Ashman, P.J., Zevenhoven, M., Hupa, M., Van Eyk, P.J., De Nys, R., Karlström, O., Lewis, D.M., 2014. Combustion behavior of algal biomass: Carbon release, nitrogen release, and char reactivity. Energy and Fuels 28, 41–51. https://doi.org/10.1021/ef4014983

Lebron, Y.A.R., Moreira, V.R., Santos, L.V.S., 2019. Studies on dye biosorption enhancement by chemically modified Fucus vesiculosus, Spirulina maxima and Chlorella pyrenoidosa algae. J. Clean. Prod. 240, 118197. https://doi.org/10.1016/j.jclepro.2019.118197

Liao, J.C., Mi, L., Pontrelli, S., Luo, S., 2016. Fuelling the future: Microbial engineering for the production of sustainable biofuels. Nat. Rev. Microbiol. 14, 288–304. https://doi.org/10.1038/nrmicro.2016.32

Lichtenthaler, H.K., 1987. Chlorophylls Carotenoids. Chlorophylls Carotenoids Pigment. Photosynth. Biomembr. 148, 350–382. https://doi.org/10.1016/0076-6879(87)48036-1

Lobakova, E., Vasilieva, S., Kashcheeva, P., Ivanova, E., Dolnikova, G., Chekanov, K., Idiatulov, R., Kirpichnikov, M., Buznik, V., Dedov, A., 2016. New bio-hybrid materials for bioremoval of crude oil spills from marine waters. Int. Biodeterior. Biodegrad. 108, 99–107. https://doi.org/10.1016/j.ibiod.2015.12.016

Ma, Y., Zhao, Z., Fan, J., Gu, Z., Zhang, B., Yin, S., 2018. Ag-TON nanospheres coupled with fly ash cenospheres for wastewater treatment under visible light irradiation. Water Sci. Technol. 78, 2321–2327. https://doi.org/10.2166/wst.2018.513

Molin Filho, R.G.D., Colpini, L.M.S., Ferrer, M.M., Nagano, M.F., Rosso, J.M., Volnistem, E.A., Paraíso, P.R., de Matos Jorge, L.M., 2019. Characterization of different sugarcane bagasse ashes generated for preparation and application as green products in civil construction. Clean Technol. Environ. Policy 21, 1687–1698. https://doi.org/10.1007/s10098-019-01740-x

Naddeo, V., Belgiorno, V., Kassinos, D., Mantzavinos, D., Meric, S., 2010. Ultrasonic degradation, mineralization and detoxification of diclofenac in water: Optimization of operating parameters. Ultrason. Sonochem. 17, 179–185. https://doi.org/10.1016/j.ultsonch.2009.04.003

Pignatello, J.J., Oliveros, E., MacKay, A., 2006. Advanced oxidation processes for organic contaminant destruction based on the fenton reaction and related chemistry. Crit. Rev. Environ. Sci. Technol. 36, 1–84. https://doi.org/10.1080/10643380500326564

Pradhan, D., Sukla, L.B., Mishra, B.B., Devi, N., 2019. Biosorption for removal of hexavalent chromium using microalgae Scenedesmus sp. J. Clean. Prod. 209, 617–629. https://doi.org/10.1016/j.jclepro.2018.10.288

Rahim Pouran, S., Abdul Raman, A.A., Wan Daud, W.M.A., 2014. Review on the application of modified iron oxides as heterogeneous catalysts in Fenton reactions. J. Clean. Prod. 64, 24–35. https://doi.org/10.1016/j.jclepro.2013.09.013

Ramírez-Franco, J.H., Galeano, L.-A., Vicente, M.-A., 2019. Fly ash as photo-Fenton catalyst for the degradation of amoxicillin. J. Environ. Chem. Eng. 7, 103274. https://doi.org/10.1016/j.jece.2019.103274

Serrà, A., Artal, R., García-Amorós, J., Sepúlveda, B., Gómez, E., Nogués, J., Philippe, L., 2019. Hybrid Ni@ZnO@ZnS-Microalgae for Circular Economy: A Smart Route to the Efficient Integration of Solar Photocatalytic Water Decontamination and Bioethanol Production. Adv. Sci. 1902447, 1–9. https://doi.org/10.1002/advs.201902447

Serrà, A., Artal, R., García-Amorós, J., Gómez, E., 2020. Circular zero-residue process using microalgae for efficient water decontamination, biofuel production, and carbon dioxide fixation. Chem. Eng. J. 124278. https://doi.org/10.1016/j.cej.2020.124278

Shanab, S.M.M., Hafez, R.M., Fouad, A.S., 2018. A review on algae and plants as potential source of arachidonic acid. J. Adv. Res. 11, 3–13. https://doi.org/10.1016/j.jare.2018.03.004

Singh, J.S., Kumar, A., Rai, A.N., Singh, D.P., 2016. Cyanobacteria: A precious bio-resource in agriculture, ecosystem, and environmental sustainability. Front. Microbiol. 7, 1–19. https://doi.org/10.3389/fmicb.2016.00529

Solovchenko, A., Pogosyan, S., Chivkunova, O., Selyakh, I., Semenova, L., Voronova, E., Scherbakov, P., Konyukhov, I., Chekanov, K., Kirpichnikov, M., Lobakova, E., 2014. Phycoremediation of alcohol distillery wastewater with a novel Chlorella sorokiniana strain cultivated in a photobioreactor monitored on-line via chlorophyll fluorescence. Algal Res. 6, 234–241. https://doi.org/10.1016/j.algal.2014.01.002

Tosti, L., van Zomeren, A., Pels, J.R., Damgaard, A., Comans, R.N.J., 2019. Life cycle assessment of the reuse of fly ash from biomass combustion as secondary cementitious material in cement products. J. Clean. Prod. https://doi.org/10.1016/j.jclepro.2019.118937

Tsegaye, B., Balomajumder, C., Roy, P., 2019. Organosolv pretreatments of rice straw followed by microbial hydrolysis for ef fi cient biofuel production. Renew. Energy. https://doi.org/10.1016/j.renene.2019.10.176

Wellburn, A.R., Lichtenthaler, H., 1984. Formulae and Program to Determine Total Carotenoids and Chlorophylls A and B of Leaf Extracts in Different Solvents, in: Sybesma, C. (Ed.), Advances in Photosynthesis Research: Proceedings of the VIth International Congress on Photosynthesis, Brussels, Belgium, August 1--6, 1983 Volume 2. Springer Netherlands, Dordrecht, pp. 9–12. https://doi.org/10.1007/978-94-017-6368-4_3

Wong, S., Ngadi, N., Inuwa, I.M., Hassan, O., 2018. Recent advances in applications of activated carbon from biowaste for wastewater treatment: A short review. J. Clean. Prod. 175, 361–375. https://doi.org/10.1016/j.jclepro.2017.12.059

Wong, S., Ngadi, N., Inuwa, I.M., Hassan, O., 2018. Recent advances in applications of activated carbon from biowaste for wastewater treatment: A short review. J. Clean. Prod. 175, 361–375. https://doi.org/10.1016/j.jclepro.2017.12.059

Yadav, L.S., Mishra, B.K., Kumar, A., Paul, K.K., 2014. Arsenic removal using bagasse fly ash-iron coated and sponge iron char. J. Environ. Chem. Eng. 2, 1467–1473. https://doi.org/10.1016/j.jece.2014.06.019

Zarrouk, C., 1966. Contribution a l'etude d'une cyanobacterie: influence de divers facteurs physiques et chimiques sur la croissance et la photosynthese de Spirulina maxima (Setchell et Gardner) Geitler. University of Paris, Paris.

Zeghioud, H., Khellaf, N., Djelal, H., Amrane, A., Bouhelassa, M., 2016. Photocatalytic Reactors Dedicated to the Degradation of Hazardous Organic Pollutants: Kinetics, Mechanistic Aspects, and Design – A Review. Chem. Eng. Commun. 203, 1415–1431. https://doi.org/10.1080/00986445.2016.1202243

Zelelew, D., Gebrehiwot, H., Fikre, W., 2018. Feasibility of Bioethanol Production Potential and Optimization from Selected Lignocellulosic Waste Biomass 13, 53–67.

Zhang, C., Show, P.L., Ho, S.H., 2019. Progress and perspective on algal plastics – A critical review. Bioresour. Technol. 289, 121700. https://doi.org/10.1016/j.biortech.2019.121700

Zhang, J., Li, J., Thring, R., Liu, L., 2013. Application of Ultrasound and Fenton's Reaction Process for the Treatment of Oily Sludge. Procedia Environ. Sci. 18, 686–693. https://doi.org/10.1016/j.proenv.2013.04.093

Zhao, T., Tashiro, Y., Sonomoto, K., 2019. Smart fermentation engineering for butanol production: designed biomass and consolidated bioprocessing systems. Appl. Microbiol. Biotechnol. https://doi.org/10.1007/s00253-019-10198-2